HURP permits MTOC sorting for robust meiotic spindle bipolarity, similar to extra centrosome clustering in cancer cells

Manuel Breuer,[1] Agnieszka Kolano,[1] Mijung Kwon,[2] Chao-Chin Li,[3] Ting-Fen Tsai,[3] David Pellman,[2] Stéphane Brunet,[1] and Marie-Hélène Verlhac[1]

[1]Unité Mixte de Recherche 7622, Centre National de la Recherche Scientifique/Université Pierre et Marie Curie, 75005 Paris, France
[2]Howard Hughes Medical Institute, Department of Pediatric Oncology, Dana-Farber Cancer Institute, Harvard Medical School, Boston, MA 02115
[3]Department of Life Sciences and Institute of Genome Sciences, National Yang-Ming University, Taipei 112, Taiwan

In contrast to somatic cells, formation of acentriolar meiotic spindles relies on the organization of microtubules (MTs) and MT-organizing centers (MTOCs) into a stable bipolar structure. The underlying mechanisms are still unknown. We show that this process is impaired in *hepatoma up-regulated protein* (*Hurp*) knockout mice, which are viable but female sterile, showing defective oocyte divisions. HURP accumulates on interpolar MTs in the vicinity of chromosomes via Kinesin-5 activity. By promoting MT stability in the spindle central domain, HURP allows efficient MTOC sorting into distinct poles, providing bipolarity establishment and maintenance. Our results support a new model for meiotic spindle assembly in which HURP ensures assembly of a central MT array, which serves as a scaffold for the genesis of a robust bipolar structure supporting efficient chromosome congression. Furthermore, HURP is also required for the clustering of extra centrosomes before division, arguing for a shared molecular requirement of MTOC sorting in mammalian meiosis and cancer cell division.

Introduction

During meiosis, the assembly of a microtubule (MT)-based bipolar spindle is essential for the formation of a competent egg, capable upon fertilization of generating viable offspring. The spindle ensures accurate chromosome segregation to prevent aneuploidy of the embryo. It also defines the cell division plane, leading to the formation of a large egg and a tiny polar body. In most species, meiotic spindles lack canonical centrosomes. Instead, the formation of a bipolar spindle results from organization of MTs and, in vertebrates, from multiple, discrete MT-organizing centers (MTOCs) around chromosomes (Dumont et al., 2007; Schuh and Ellenberg, 2007). Little is known about the mechanisms that govern the MT-MTOC reorganization into a bipolar structure. This is partly because of the lack of genetic studies on meiotic spindle organization using loss-of-function mutants in vertebrates. To characterize molecular factors involved in meiotic spindle assembly, we have started to analyze spindle assembly factors of knockout mice that are viable but female sterile, potentially caused by essential functions in meiotic divisions. Using this strategy, we have identified hepatoma up-regulated protein (HURP) as a key meiotic factor. HURP is an MT-associated protein and a Ran GTPase effector previously identified for its function in mitotic kinetochore fiber stability. However, it is dispensable for mitosis completion (Koffa et al., 2006; Silljé et al., 2006). Here, we show that HURP, via its local concentration by activity of the Kinesin-5 motor, is required for the assembly of a robust central MT domain, itself allowing the establishment and maintenance of meiotic spindle bipolarity. This domain acts as a scaffold for the accurate sorting of MTOCs to spindle poles and serves to congress chromosomes toward the spindle equator. This new function for HURP sheds light on the complex architecture of the female meiotic spindle. Moreover, by extending our study to cancer cells bearing multiple centrosomes (Godinho et al., 2009),

Correspondence to Stéphane Brunet: stephane.brunet@snv.jussieu.fr; or Marie-Hélène Verlhac: marie-helene.verlhac@upmc.fr

Abbreviations used in this paper: HURP, hepatoma up-regulated protein; MT, microtubule; MTOC, MT-organizing center; NEBD, nuclear envelope breakdown; wt, wild type.

The Rockefeller University Press $30.00
J. Cell Biol. Vol. 191 No. 7 1251–1260
www.jcb.org/cgi/doi/10.1083/jcb.201005065

we present evidence that the genetic requirement for meiosis and the pathways used by some tumors to divide might be evolutionarily shared.

Results and discussion

Hurp deficiency specifically impairs completion of meiotic divisions in oocytes

Knockout mice for *Hurp* were found to be viable but female sterile, indicating that HURP is dispensable for mitosis (Tsai et al., 2008). We reasoned that the sterility could be caused by abnormal oocyte meiotic divisions giving rise to aneuploid embryos upon fertilization. Therefore, we analyzed meiotic progression of oocytes collected from $Hurp^{-/-}$ females. Although HURP is expressed at a constant level in maturing wild-type (wt) oocytes (Fig. 1 A), $Hurp^{-/-}$ females harbor undetectable levels of the protein, confirming a true knockout (Fig. 1 B). Most *wt* oocytes extrude their first polar body 9 h after nuclear envelope breakdown (NEBD; Fig. 1 C). In contrast, 12 h after NEBD, only 50% of *Hurp*-deficient oocytes extruded their polar bodies (Fig. 1 C). Associated with this delay, chromosome dynamics were altered. Homologous chromosomes neither congressed properly nor formed a proper metaphase plate (Fig. 1 D, Video 1, and Video 2). More than 60% of $Hurp^{-/-}$ oocytes exhibited lagging chromosomes at anaphase (Fig. 1 D, arrow; Fig. 2 A; Video 4; and Video 5). Chromosome spreads performed on metaphase II (MII) oocytes showed that $Hurp^{-/-}$ oocytes contained univalents (unpublished data), indicative of normal separase activation at anaphase I (Terret et al., 2003b; Kudo et al., 2006). After polar body extrusion, chromosomes were scattered in MII (Fig. 1 E). Chromosome dynamics were rescued by expressing GFP-HURP, again confirming a specific knockout in this strain (Fig. 1 E). HURP is thus a key factor of oocyte meiotic divisions, whereas it is dispensable for mitosis: it is required for timed meiotic progression and proper segregation of homologous chromosomes. In its absence, nonfunctional female gametes are formed, leading to female sterility (Tsai et al., 2008).

HURP localizes to a central domain of the meiotic spindle

HURP localization and dynamics were then analyzed in maturing oocytes. At NEBD, multiple MTOCs and associated MTs surround the chromosomes to organize into a bipolar spindle. At this stage, HURP was enriched on MTs assembled between MTOCs and chromosomes (Fig. 1 F and Fig. S1 A). After spindle bipolarization, HURP was restricted to the central domain of MI and MII spindles (Fig. 1 F). Such localization, lost in $Hurp^{-/-}$ oocytes (Fig. S1 C), was also observed for GFP-tagged HURP (Fig. 1 G, Fig. S1 B, and Video 3). As expected, HURP localization was abolished upon MT depolymerization and expression of a dominant-negative Ran mutant (Fig. S1, D and E). In mitosis, HURP is considered to be a marker of kinetochore fibers (Koffa et al., 2006; Silljé et al., 2006). In oocytes, HURP could be observed on MTs emanating from the kinetochores only at the end of MI and in MII (Fig. 1 H). Strikingly, during MI, HURP was associated with nonkinetochore MTs crossing the spindle equator, reminiscent of interpolar MTs (Fig. 1 H). This is consistent with the formation of stable K fibers only at the end of MI (Brunet et al., 1999) and suggested that HURP performs additional functions during meiosis, which were not anticipated from studies in mitosis (Silljé et al., 2006; Wong and Fang, 2006).

Hurp deficiency affects the setting up of meiotic spindle bipolarity

Meiotic spindle assembly in the absence of HURP was analyzed by time-lapse spinning-disk microscopy using EB3-GFP, a well-characterized MT plus-end marker, which was previously used in mouse oocytes (Schuh and Ellenberg, 2007). It gives a strong signal throughout the spindle, presumably caused by short MTs of mixed polarity, which are abundant in meiotic spindles (Srayko et al., 2006; Yang et al., 2007; Liang et al., 2009). In *wt*, at NEBD, multiple MTOCs and MTs formed evenly distributed asters associated with chromosomes (Fig. 2 A), which were sorted into a bipolar structure 3.5 h later (Fig. 2 C). In contrast, in $Hurp^{-/-}$ oocytes, spindle assembly was impaired (Fig. 2 A). After NEBD, MTOCs and MTs rapidly became unevenly distributed, with chromosomes expelled to the periphery of the MT array (Fig. 2 B and Fig. S2 A). The bipolarization of such structures was nevertheless observed with a delay of 1.5 h (Fig. 2 C). Hence, HURP is required for timely bipolarization at early stages of MI.

Hurp deficiency impairs the maintenance of meiotic spindle bipolarity

In *wt* oocytes, upon bipolarization, chromosomes congressed to the spindle equator, and eventually, 9 h after NEBD on average, anaphase and chromosome segregation occurred. The second meiotic spindle then rapidly assembled and remained stable during the MII arrest (Fig. 2 A and Video 4). In 80% of $Hurp^{-/-}$ oocytes, spindles observed in MI were unsteady (Fig. 2 D). Spindle collapse, irreversible in some cases, was partially reverted in 60% of oocytes within a few hours (Fig. 2 D and Video 6). To quantify this, spindle lengths were scored throughout 17 h of meiotic maturation (Fig. 2 E). In $Hurp^{-/-}$ oocytes, the mean spindle length was significantly reduced compared with *wt* (18.54 ± 2.62 µm vs. 26.42 ± 3.18 µm, respectively; Fig. 3 A). Remarkably, although size was stable in controls (Fig. 2 E, green curve), it varied over time in $Hurp^{-/-}$ oocytes, even for spindles reaching the expected spindle length (Fig. 2 E, red curves). Therefore, HURP is required for establishment and maintenance of meiotic spindle bipolarity.

HURP promotes MT stability in the central region of the spindle

We then measured relative MT densities using EB3-GFP. At NEBD, both *wt* and $Hurp^{-/-}$ oocytes exhibited comparable MT densities. However, the density of MTs increased with time in *wt* but remained steady in the *Hurp* deficiency (Fig. 3 A). Similarly, 2 h after NEBD, in oocytes treated with monastrol to inhibit bipolarization, the density of MTs was lower, and monasters were smaller in $Hurp^{-/-}$ oocytes compared with *wt* (Fig. 3 B). These differences were not caused by disparities in EB3-GFP expression (Fig. S3, C and D). Using individual MT tracking, we did not observe significant differences in MT growth rates at NEBD (Fig. S3 A) or 2 h

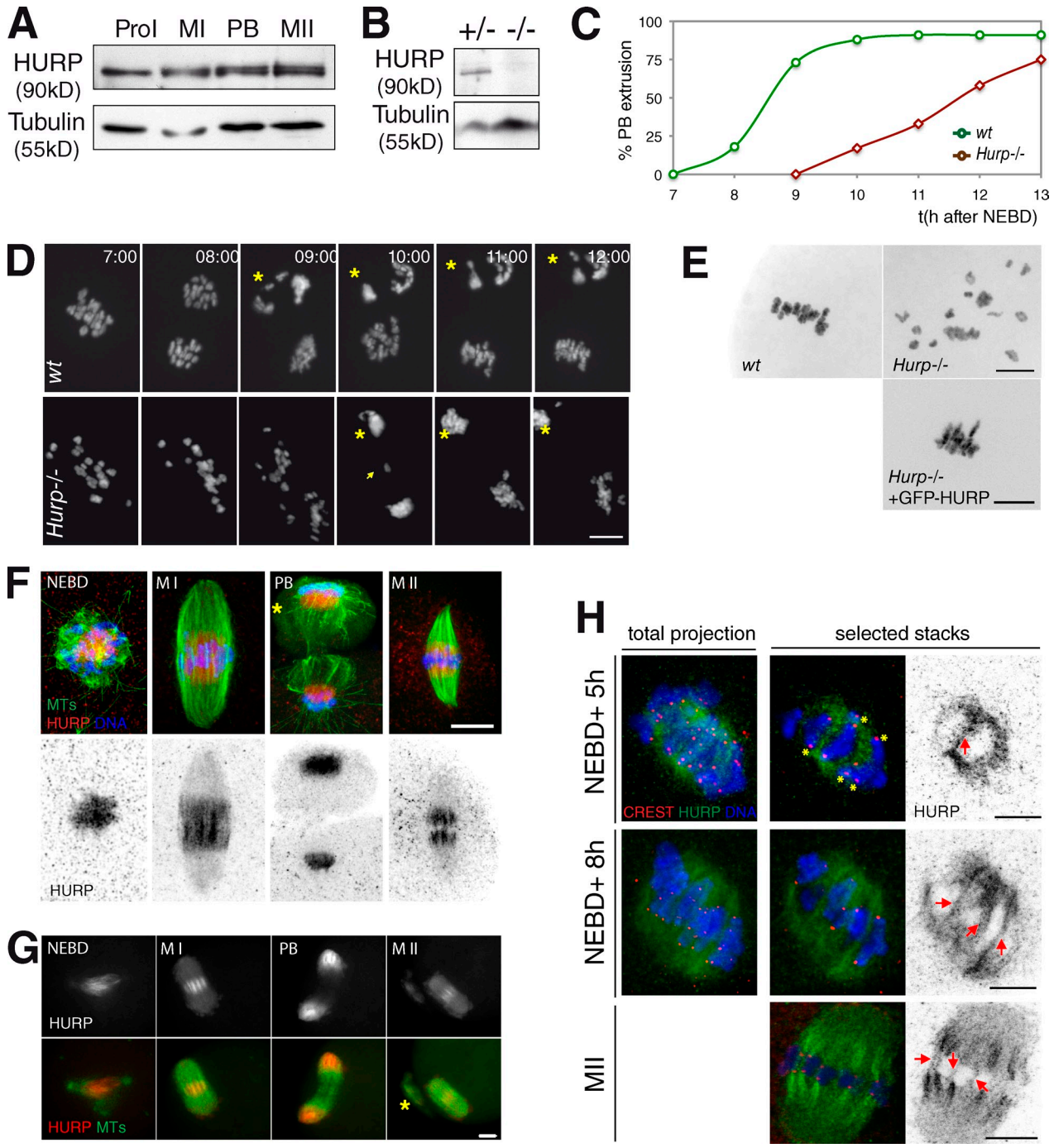

Figure 1. ***Hurp*$^{-/-}$ oocytes present late anaphases and lagging chromosomes and spread MII plates.** (A) HURP levels are constant during meiotic maturation. Oocytes were collected in prophase I (ProI), 4 h after NEBD (MI), during polar body (PB) extrusion, and during MII. (B) HURP is absent in liver extracts from *Hurp*$^{-/-}$ mice. (C) Percentage of first polar body extrusion over time in *wt* versus *Hurp*$^{-/-}$ oocytes. (D) Aberrant bivalent separation in *Hurp*$^{-/-}$ oocytes. (top) *wt* with normal chromosome separation. (bottom) *Hurp*$^{-/-}$ with lagging chromosomes (arrow) and delayed anaphase I, both expressing H2B-RFP. Asterisks, polar bodies. All times are given in hours and minutes after NEBD. (E) *Hurp*$^{-/-}$ oocytes present disorganized MII plates, which were rescued by HURP expression. Chromosomes in MII from *wt* (top left), *Hurp*$^{-/-}$ (top right), and *Hurp*$^{-/-}$ oocytes expressing GFP-HURP (bottom). (F) HURP localizes in the vicinity of chromosomes in the spindle midzone. Oocytes stained with Hoechst (blue), tubulin (green), and HURP. Asterisk, polar body. (G) GFP-HURP behaves like endogenous protein. Oocytes are shown expressing EB3-mCherry (green) and GFP-HURP. Maximal Z projections are shown. Asterisk, polar body. (H) HURP does not label K fibers in prometaphase I. Oocytes were stained at NEBD + 5 h (prometaphase I), NEBD + 8 h (MI), and MII with Hoechst; CREST for kinetochores; and HURP. Maximum projections or selected stacks are shown. Asterisks, kinetochore MTs not decorated by HURP. Arrows, HURP on interpolar MTs. Bars, 10 µm.

later upon monastrol treatment, which facilitated MT tracking at this stage (Fig. S3 B). Thus, HURP does not promote MT growth but rather MT stability around chromosomes.

We also analyzed MT density along the spindle axis later in MI. In *wt*, the density of MTs culminates in the spindle equator where HURP accumulates and where interpolar MTs

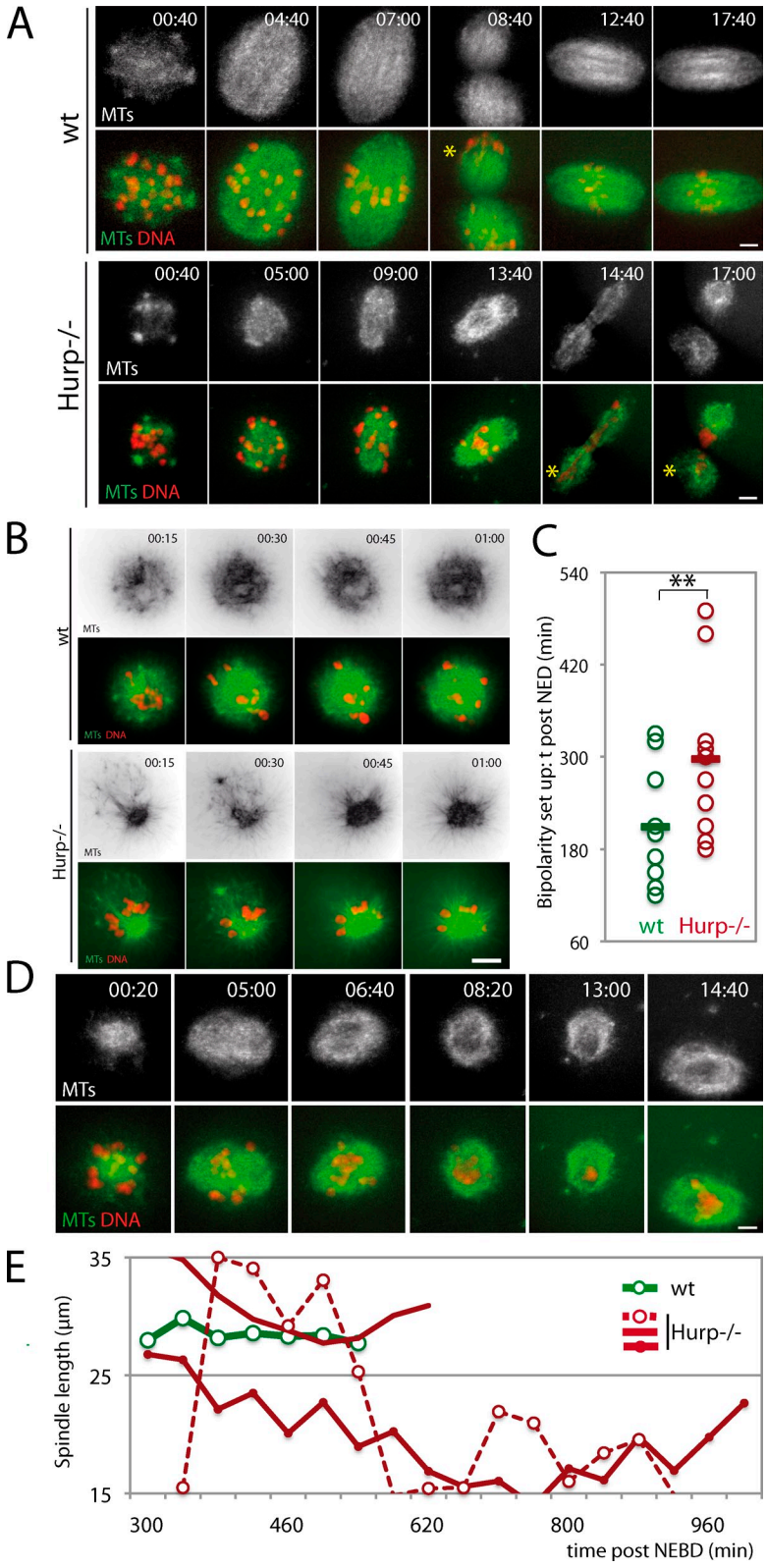

Figure 2. ***Hurp*$^{-/-}$ oocytes are delayed in bipolarization and undergo spindle collapse.** (A) *Hurp*$^{-/-}$ oocytes present spindle defects. For A, B, and D, oocytes express EB3-GFP (green) and H2B-RFP (red). Asterisks, polar bodies. (B) MTs are not evenly distributed around chromosomes after NEBD in *Hurp*$^{-/-}$. Mean projections of 10 Z planes are shown. (C) Setup of spindle bipolarity is delayed in *Hurp*$^{-/-}$ oocytes. Bipolarity was scored when two poles were distinguishable. It is delayed in *Hurp*$^{-/-}$ oocytes, starting at 297 ± 101 min instead of 209 ± 74 min (**, P = 0.0334). Lines indicate the mean time for bipolarity setup. (D) Transient spindle collapse in *Hurp*$^{-/-}$ oocytes during MI. Bipolarity reappears at 14 h and 40 min after NEBD. (E) Unstable spindle length in *Hurp*$^{-/-}$ oocytes. Length was determined by longitudinal line scans of images from *wt* (n = 12) and *Hurp*$^{-/-}$ (n = 14) oocytes. Representative curves are shown. All times are given in hours and minutes after NEBD. Bars, 10 µm.

do overlap (Fig. 3 C, top). In contrast, MT density was lowest in this region in *Hurp*$^{-/-}$ oocytes (Fig. 3 C, bottom). Therefore, after bipolarization, the reduction of MT density is restricted to the central domain of the spindle in these oocytes. Collectively, HURP promotes the organization of MTs into a robust midzone.

Hurp is required for MTOC sorting toward spindle poles

In oocytes lacking centrosomes, spindle assembly depends on the poorly understood self-organization of MTOCs and MTs around chromosomes. We characterized MTOC dynamics during MI. 2 h after NEBD, upon bipolarization, MTOCs were

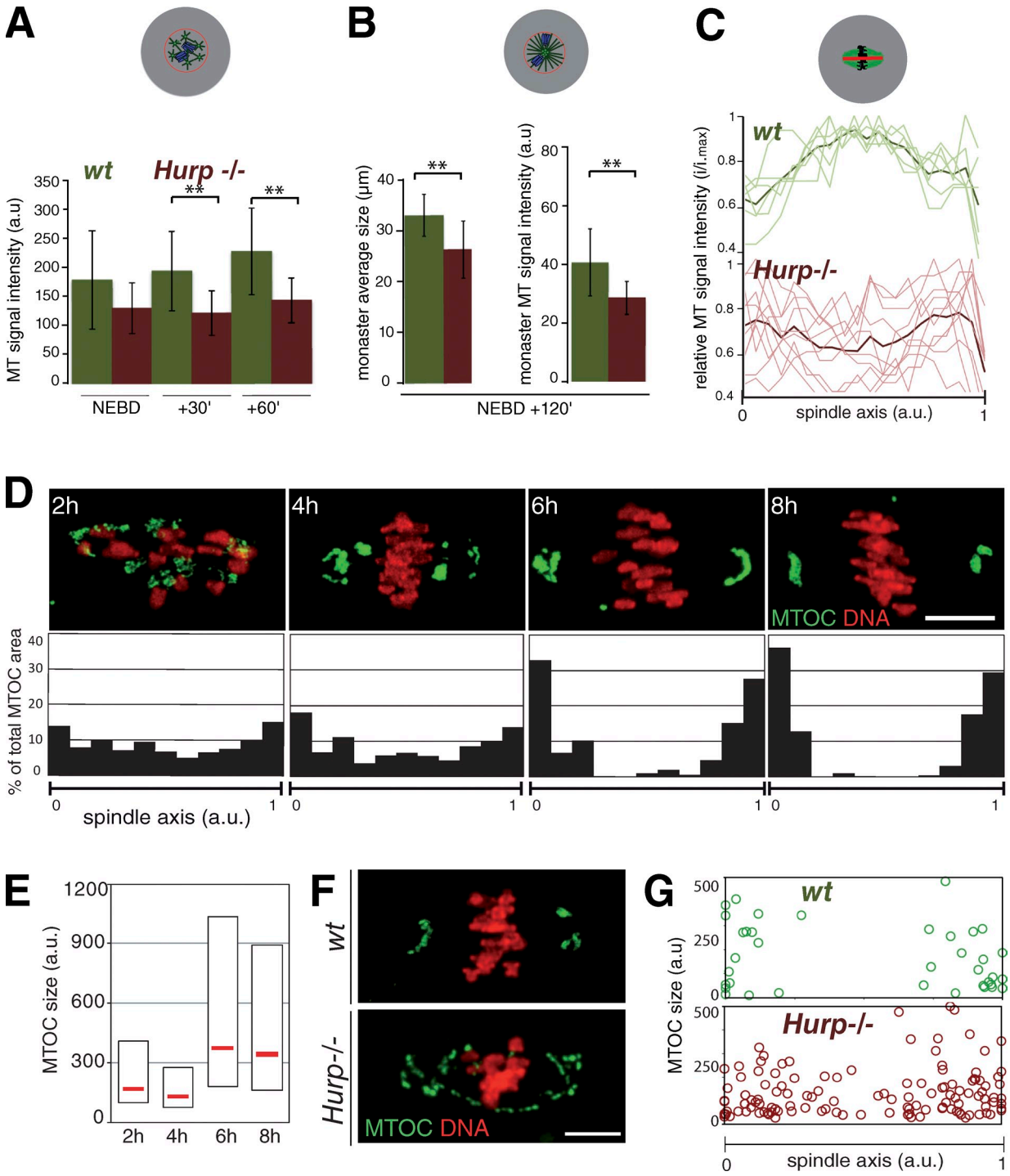

Figure 3. ***Hurp*$^{-/-}$ oocytes show reduced MT density and improper MTOC distribution.** (A) Reduced MT density early on in *Hurp*$^{-/-}$ oocytes. Fluorescence intensity in *wt* and *Hurp*$^{-/-}$ oocytes, expressing EB3-GFP and H2B-RFP, was assessed in the chromosome vicinity. MT density is lower in *Hurp*$^{-/-}$ oocytes (n = 9) from NEBD + 30 and + 60 min (**, P = 0.0125 and 0.0071) compared with *wt* (n = 10). (B) Prometaphase I monasters are smaller, with fewer MTs in *Hurp*$^{-/-}$ oocytes. Fluorescence intensity was assessed as in A in monastrol-treated oocytes at NEBD + 2 h. Mean monaster size: 29.19 ± 3.04 µm for *Hurp*$^{-/-}$ compared with 32.86 ± 2.22 µm for *wt* (left; **, P = 0.0143). Monaster MT density is lower in *Hurp*$^{-/-}$ than *wt* (right histogram; *wt*, n = 9; and *Hurp*$^{-/-}$, n = 7; **, P = 0.0228). Error bars represent standard deviation. (C) Low MT density in the spindle center in *Hurp*$^{-/-}$ oocytes. Longitudinal line scans from MI spindles of *wt* (n = 6) and *Hurp*$^{-/-}$ (n = 10). Intensities were normalized to maximum value within the same spindle, and spindle size was interpolated. Light curves, individual spindles. Dark curves, mean values. (D) MTOCs are progressively sorted at spindle poles in MI. (top) MTOCs were labeled using pericentrin (green) and chromosomes with Hoechst (red). (bottom) Quantitative analysis of MTOC distribution along the spindle axis at 2 (n = 16), 4 (n = 18), 6 (n = 22), and 8 h (n = 17) after NEBD. The pericentrin signal was binarized to assess the individual MTOC area (a.u., arbitrary units). Coordinates of MTOCs are plotted along the spindle axis (0–1). (E) MTOCs are progressively clustered during MI. Box plot representation of individual MTOC size at selected time points. Median values are shown in red. (F) Abolished MTOC sorting in *Hurp*$^{-/-}$ oocytes. *wt* and *Hurp*$^{-/-}$ oocytes were observed at NEBD + 7 h and labeled as in D. (G) Quantification of MTOC distribution along the spindle axis in late MI in *wt* (n = 5) versus *Hurp*$^{-/-}$ (n = 10). Pericentrin signal was binarized as in D. Individual MTOC size is plotted against its coordinates on the spindle axis (0–1). Bars, 10 µm.

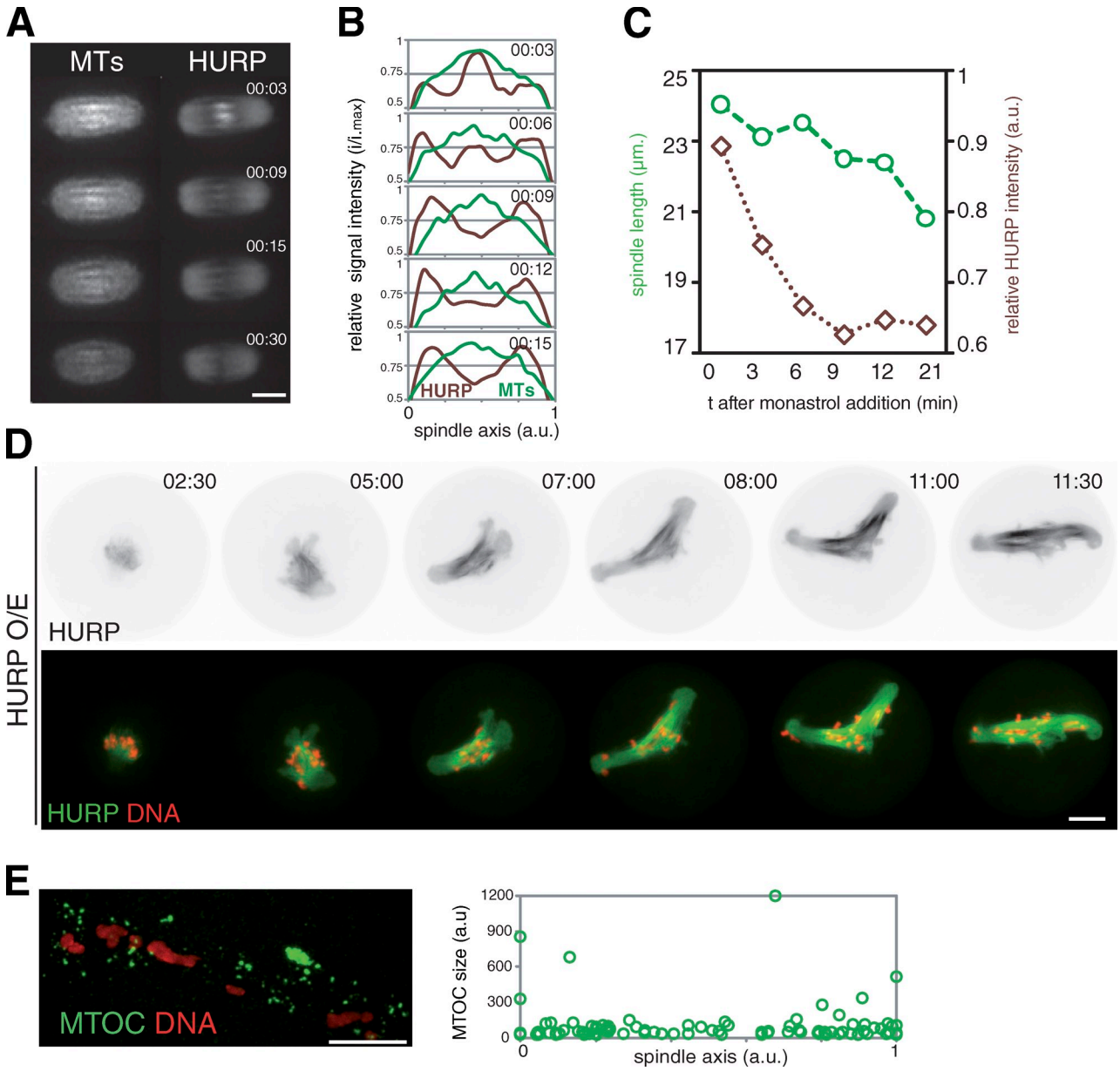

Figure 4. **Kinesin-5 recruits HURP to the spindle midzone for robust spindle bipolarity.** (A) Loss of HURP accumulation in the central region upon Kinesin-5 inhibition. MII oocytes are shown after monastrol addition, expressing EB3-mCherry (left) and GFP-HURP (right). (B) Longitudinal line scan from oocytes observed in A. Intensity was normalized, and spindle length was interpolated (n = 5). (C) Representative spindle length and relative intensity of HURP fluorescence after monastrol addition. (D) HURP overexpression promotes central spindle assembly and perturbs spindle bipolarization and chromosome congression. GFP-HURP overexpression (see Materials and methods) affects spindle formation and MI division (noninjected: 100% polar body, n = 41; and GFP-HURP overexpression: 7% polar body, n = 67). (E) HURP overexpression disrupts MTOC clustering. Oocytes overexpressing HURP were labeled for DNA and MTOCs (pericentrin, green). (right) Quantification as in Fig. 3 G (n = 5). a.u., arbitrary units. All times are given in hours and minutes after NEBD. Bars, 10 µm.

scattered along the entire spindle axis (Fig. 3 D). Subsequently, they were targeted toward spindle extremities forming larger structures (Fig. 3, D and E) and were clustered at spindle poles by 6 h after NEBD (Fig. 3 D). The sorting and clustering were achieved long after a bipolar structure was visible (3.5 h after NEBD; Fig. 2 C). This indicates that robust spindle bipolarization relies on progressive outward sorting of MTOCs. Although at NEBD in *Hurp*$^{-/-}$ oocytes, MTOC distribution was similar to *wt* (Fig. S2, A and B), it was impaired later on (Fig. 3, F and G). Thus, HURP allows efficient sorting of MTOCs toward the poles.

Kinesin-5 activity is required to recruit HURP to the central region of the spindle

Kinesin-5 is a key motor protein for bipolarity setup of mitotic and meiotic spindles (Sawin et al., 1992; Walczak et al., 1998; Mailhes et al., 2004). HURP and Kinesin-5 are part of a large molecular complex (Koffa et al., 2006). We observed Kinesin-5 accumulation close to chromosomes before spindle bipolarization (Fig. S3 E) and on interpolar MTs (Fig. S3 E, red arrows). This indicated that Kinesin-5 and HURP localized similarly, potentially acting synergistically to support bipolarity. To test

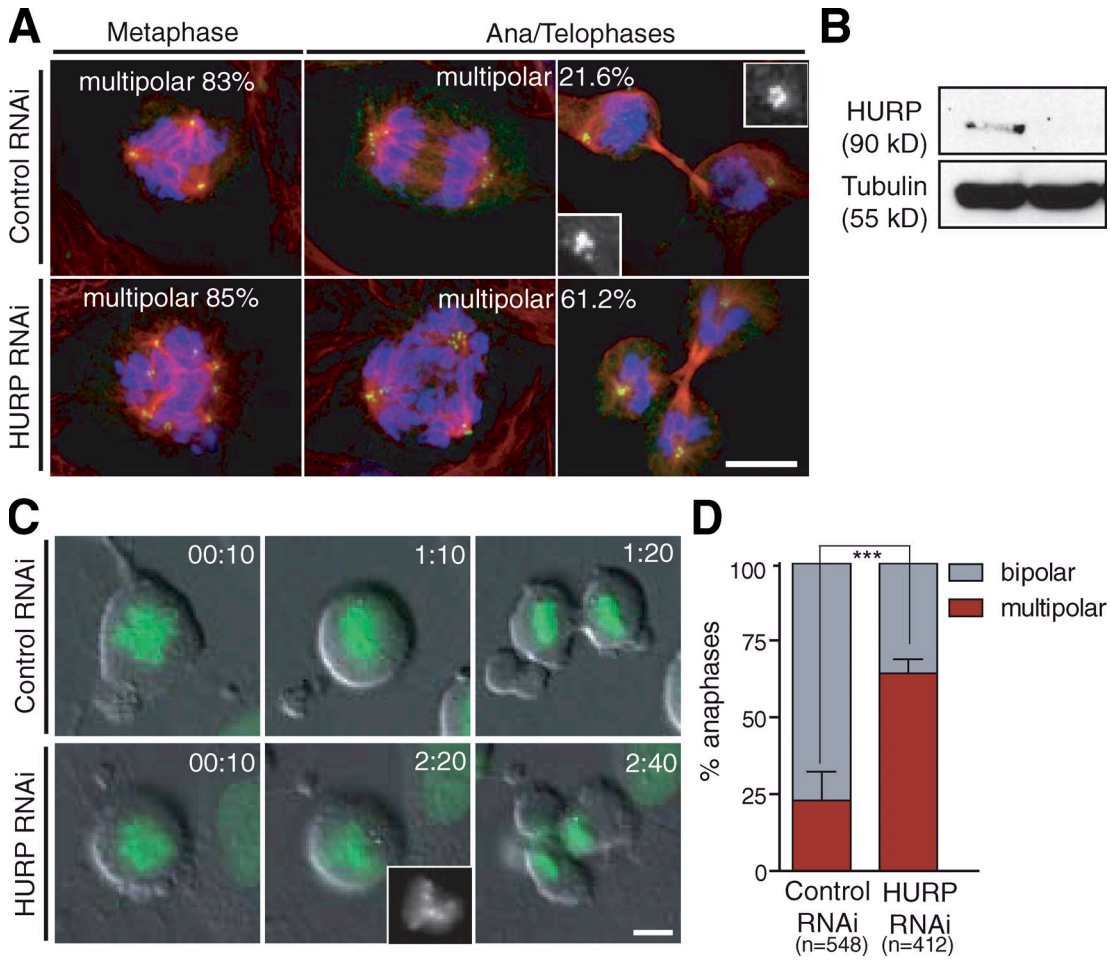

Figure 5. **HURP is required for clustering extra centrosomes in U2OS cells.** (A) HURP RNAi induces defects in clustering of extra centrosomes in cancer cells. PLK4-overexpressing U2OS cells (see Materials and methods) treated with control (luciferase) or HURP RNAi and stained for α-tubulin (red), centrin (green), and DNA (blue). (top) Control cells showing transient multipolar spindles during metaphase (left), and bipolar spindles with clustered centrosomes during anaphase/telophase (middle and right). (bottom) HURP-depleted cells showing multipolar anaphase/telophase figures. Insets show enlarged views of clustered centrosomes. (B) Knockdown of HURP in U2OS cells after 3 d of RNAi shown by Western blotting. (C) Multipolar fragmentary divisions in cells with extra centrosomes after HURP depletion. U2OS cells expressing GFP-H2B after control or HURP RNAi. (top) Control cell dividing bipolar. (bottom) Cell depleted of HURP dividing in a tripolar configuration of chromosomes before anaphase (inset). Time is shown as hours and minutes from chromatin condensation as t = 0. (D) Quantification of centrosome clustering defects in cells shown in C (***, P = 0.002). Error bars represent standard deviation. Bars, 10 µm.

this, we used monastrol to inhibit Kinesin-5. As previously reported, it induced MII spindle shortening (Fitzharris, 2009), which was associated with HURP disappearance in the central region (Fig. 4, A and B). Importantly, the decay of HURP signal was rapid and preceded spindle shortening (Fig. 4, B and C). Therefore, Kinesin-5 activity permits HURP concentration within the central domain of the meiotic spindle, which might prevent spindle shortening.

HURP overexpression disrupts meiotic spindle architecture

We investigated the effect of HURP overexpression. 93% of HURP-overexpressing oocytes ($n = 67$) remained blocked in MI with aberrant spindles. Spindles elongated with time, exhibiting a dense central array of MTs (Fig. 4 D and Video 7). Chromosomes failed to congress, being redistributed along the spindle axis. Spindle defects caused by HURP overexpression mirrored the ones of the deficiency, strengthening the importance of HURP in proper meiotic spindle architecture. Furthermore, HURP overexpression also abolished MTOC sorting and clustering to the poles (Fig. 4 E). HURP is required to organize a central array within the meiotic spindle, which permits outward sorting of MTOCs and subsequent organization of spindle poles, as well as proper control of spindle length. All these parameters contribute to the definition of a robust bipolar spindle. The central array seems to favor homologue chromosome congression (Fig. S3 F).

HURP has a critical role in the clustering of extra centrosomes during mitosis in human cancer cells

The process of bipolar spindle assembly in the presence of multiple MTOCs in female meiosis resembles the clustering of extra centrosomes during cancer cell division. We hypothesized that the presence of extra centrosomes could impose an essential role of HURP in cancer cell division, which requires centrosome

clustering. To test this, we characterized mitosis in U2OS cells, in which centrosomes are overduplicated by overexpressing PLK4 (Kleylein-Sohn et al., 2007) after HURP RNAi. In controls, despite extra centrosomes, the majority of cells (~80%) successfully divide because of efficient clustering of extra centrosomes before anaphase (Fig. 5 A, top). The percentage of cells with transient multipolar spindle intermediates is similar in control versus HURP-depleted cells (Fig. 5 A, left). However, HURP knockdown results in a drastic increase in multipolar spindles in postanaphase cells (Fig. 5 A, bottom). 61.2% of HURP-depleted extracentrosomal cells ($n = 262$) display multipolar ana/telophase figures compared with 21.6% in controls ($n = 164$). Consistently, following live U2OS cells revealed that HURP knockdown induced an increase in fragmentary multipolar anaphases (64.25 ± 2.3% in HURP RNAi vs. 22.93 ± 4.7% in controls; Fig. 5, C and D; Video 8; and Video 9). Our data suggest that HURP has a conserved role in MTOC organization and assembly of bipolar spindles in both oocytes and cancer cells with extra centrosomes.

In mitosis, HURP stabilizes K fibers but is dispensable. In contrast, we show that HURP is an essential meiotic spindle assembly factor. It associates with MTs and is enriched in the vicinity of chromosomes, where it promotes the assembly of a central MT array. This structure in turn allows the outward sorting of MTOCs to the poles. Through an original inside-out mechanism, HURP, possibly via Kinesin-5 activity, controls the formation and maintenance of a robust bipolar acentriolar spindle (Fig. S3 F). Interestingly, this central array is also important for proper chromosome alignment on the spindle equator, in agreement with previous findings that, in meiosis, chromosome congression does not rely on K fibers (Brunet et al., 1999; Wignall and Villeneuve, 2009). Oocytes undergo extremely asymmetric divisions in size. Losing canonical centrosomes seems to be a common strategy to minimize the size of polar bodies: lacking astral MTs, the distance between one spindle pole to the plasma membrane is reduced. One consequence of losing this powerful engine for astral MT assembly is a strong actin-based spindle positioning (Azoury et al., 2008; Schuh and Ellenberg, 2008). Another consequence might be the assembly of a robust central domain, based on chromosome-mediated MT assembly. A prominent central array of MTs has been reported for meiotic spindles assembled in *Xenopus laevis* egg extracts (Yang et al., 2008) and in *Drosophila melanogaster* oocytes, where it also depends on the activities of an MT-associated protein, INCENP (inner centromeric protein), and on a kinesin-like protein, Subito (Colombié et al., 2008). In mitotic cells, this meiotic mode of spindle assembly is probably present but dominated by other mechanisms, as previously demonstrated for the Kinesin-14 Ncd/HSET (nonclaret disjunctional/human spleen embryo and testes; Kwon et al., 2008). Indeed, we present evidence that bundling extra centrosomes in cancer cells reveals a latent meiotic-like program. The mechanisms of MTOC sorting in mouse oocytes share similarities with properties of some cancer cells, which cluster extra centrosomes before division to ensure bipolarity and thus viability (Kwon et al., 2008). The role of HURP in these two processes is conserved, yet further investigations are needed to demonstrate that the mechanisms at play are shared. HURP was first identified as being up-regulated in hepatocellular carcinomas (Tsou et al., 2003), solid tumors characterized by the presence of multiple centrosomes and often of clonal origin (Yao and Mishra, 2009). Therefore, it is tempting to speculate that the essential meiotic and oncogenic function of HURP originates from an evolutionarily conserved stem cell–ness.

Materials and methods

Mouse oocyte collection, culture, and microinjection

Collection of oocytes from OF1 and BL129 (*Hurp*$^{+/-}$ and *Hurp*$^{-/-}$; Tsai et al., 2008) mice was performed as previously described (Brunet and Maro, 2007), and prophase I arrest was ensured by adding 1 µM milirinone (Reis et al., 2006) to the M2 + BSA medium. The in vitro synthesized cRNAs were injected into the oocyte cytoplasm using an Eppendorf microinjector (FemtoJet), and oocytes were further kept for 2–3 h in the prophase I arrest to allow expression of fusion proteins. Resumption of meiosis as indicated by NEBD was triggered upon transfer of oocytes into a milirinone-free M2 + BSA medium. Nocodazole and monastrol were used at 10 µM and 100 µM, respectively, in M2 + BSA. All live cultures and imaging were performed at 37°C.

Plasmid construction and in vitro transcription of synthetic RNA

The murine HURP cDNA (provided by A.P. Tsou, National Yang-Ming University, Taipei, Taiwan) was subcloned into pRN3-mCherry and pRN3-GFP. The pRN3 plasmids containing RanWT, RanT24N, RanQ69L, and Histone-2BRFP have been previously described (Tsurumi et al., 2004; Dumont et al., 2007). The EB3 comes from the human cDNA (gift from F. Nothias, Université Pierre et Marie Curie, Paris, France) and was subcloned into pRN3-mCherry and pRN3-GFP. In vitro synthesis of capped cRNA was performed as previously described (Verlhac et al., 2000). For GFP-HURP overexpression, cRNA were further poly-A tailed using the Poly(A) Tailing kit (Applied Biosystems) according to the manufacturer's instructions before purification.

Immunofluorescence

Immunofluorescence on mouse oocytes was performed as previously described (Kubiak et al., 1992). Rabbit α–murine HURP (sc-98809; Santa Cruz Biotechnology, Inc.) was used at 1:50. Rat monoclonal antibody against tyrosinated α-tubulin (YL 1/2; Abcam) was used at 1:200. Human α-CREST was used at 1:60. Mouse antipericentrin (BD) was used at 1:400. After primary antibodies were added and subsequent washes were performed, oocytes were labeled with the corresponding secondary antibodies (Jackson ImmunoResearch Laboratories, Inc.). Chromatin was labeled either with 5 µg/ml Hoechst (Invitrogen) or 10 µg/ml DAPI (Sigma-Aldrich). Image acquisition of fixed oocytes was performed on a confocal microscope (SP5/AOBS; Leica) equipped with a Plan Apochromat 63×/1.4 NA objective. 30 confocal sections, every 0.5 µm, were taken and then displayed as a maximal Z projection.

Immunofluorescence on U2OS cells was performed as previously described (Kwon et al., 2008), and images were collected by a microscope (Axiovert; Carl Zeiss, Inc.) equipped with a spinning-disk confocal head (CSU-22; Yokogawa) and a Plan Apochromat 100×/1.4 NA oil objective using SlideBook software (Intelligent Imaging Innovations). 3D images were taken with a 0.3-µm step size and then displayed as a maximal Z projection.

Immunoblotting

Immunoblotting of mouse oocytes was performed as described previously (Terret et al., 2003a). 50 oocytes were loaded per lane. Protein extracts were made from livers from *Hurp*$^{+/-}$ and Hurp$^{-/-}$ mice. For U2OS cell immunoblotting, rabbit α-HURP (A300-853A; Bethyl Laboratories, Inc.) and mouse α-mouse α-tubulin (Dm1a; Sigma-Aldrich) were used at 1:1,000 and 1:2,000 dilutions, respectively.

Live confocal microscopy

Live images were taken at 37°C in M2 + BSA using a confocal microscope with a Plan Apochromat 63×/1.4 NA objective or on a microscope (DMI6000B; Leica) with a Plan Apochromat 40×/1.25 NA objective, both enclosed in a thermostatic chamber (Life Imaging Service) equipped with a charge-coupled device camera (CoolSnap HQ2; Roper Industries) coupled to a filter wheel (Sutter; Roper Industries) and a spinning disk (CSU-X1-M1; Yokogawa). MetaMorph software 7.0 (Universal Imaging) was used to collect and analyze data, and ImageJ (National Institutes of Health) was used

to analyze and process data. 10 confocal sections, every 3 µm, were taken and then displayed as a maximal Z projection.

For time-lapse imaging of doxycycline-inducible PLK4-overexpressing U2OS cells (provided by E. Nigg, University of Basel, Basel, Switzerland), cells were transfected with control (luciferase) or HURP RNAi, synchronized with thymine for 18–20 h, released to doxycycline for 10 h followed by a second thymidine treatment for an additional 18 h, and then released to medium. Long-term live-cell imaging was performed using an automated inverted microscope (TE2000E) equipped with the Perfect Focus system (Nikon) enclosed within a temperature- and CO_2-controlled environment using a 20×/0.75 NA Plan Apochromat objective lens.

siRNA

Four different oligos of siRNAs (ON-TARGETplus set of four; LQ-016846-00-0002) against human HURP/DLG7 were purchased from Thermo Fisher Scientific. Oligo target sequences of siRNA for HURP are 5′-AGACUAAGAUUGAUAACGA-3′, 5′-GUACAGAUCUGGAUGGAUU-3′, 5′-GGUCUAAACUGCAGUAAUC-3′, and 5′-UAAAGUGGGUCGUUAUAGA-3′. An siRNA duplex targeting luciferase was used as a control. Cells were transfected with Lipofectamine RNAiMAX (Invitrogen) according to the manufacturer's instructions.

Quantification analysis

The measure of MT density along the spindle axis and monastrol-induced loss of HURP fluorescence intensity was performed on oocytes expressing either EB3-GFP alone or GFP-HURP together with EB3-mCherry. Background values were measured within a region of interest outside the cell. After background subtraction, two perpendicular lines were used to measure spindle length and width and were used to perform a line scan. The fluorescence intensities were divided by the maximal value of intensity coming from the corresponding spindle and, therefore, are expressed in arbitrary units. To compare intensities of spindles varying in size, we interpolated the data to identical length intervals.

The total and local MT fluorescence signal intensities (after NEBD and at NEBD + 2 h in monastrol) were measured in oocytes expressing EB3-GFP and H2B-RFP (single confocal images). Background values were measured within a region of interest outside the cell and were subtracted before quantification. The total fluorescence intensity was measured inside a circle of a fixed size having the mean diameter of all oocytes. For the measure of local MT fluorescence intensity, a circle was drawn delimiting the region around chromosomes showing MT growth in *wt* oocytes. The mean size of this region was used to measure the corresponding fluorescence intensity in *Hurp*$^{-/-}$ oocytes, allowing us not to over- or underestimate this intensity in *Hurp*$^{-/-}$ oocytes. The same protocol was applied to measure the fluorescence intensities from monasters.

The determination of MT speed was performed using single stacks of oocytes expressing EB3-GFP using the manual tracking plugin from ImageJ. Images were taken every 250 ms over a period of 5 s. Only MT ends in focus were analyzed. Mean values for each individual MT track were processed for statistical analysis.

Normalization, correction, and fitting of the measured fluorescence intensities were performed using Excel software (Microsoft). Statistical analysis was performed using online QuickCalcs software (GraphPad Software, Inc.).

Online supplemental material

Fig. S1 shows that HURP labels MTs in the vicinity of chromosomes and is undetectable in *Hurp*-deficient oocytes, and its localization depends on the presence of MTs and RanGTP. Fig. S2 shows that MTOC distribution in *Hurp*-deficient oocytes is comparable with *wt* at very early steps of meiotic maturation. Fig. S3 shows that MT growth at NEBD is not affected in *Hurp*-deficient oocytes. Video 1 shows chromosome segregation in a *wt* oocyte. Video 2 shows lagging chromosomes at anaphase I in a *Hurp*$^{-/-}$ oocyte. Video 3 shows dynamic localization of HURP in vivo. Video 4 shows meiotic maturation in a *Hurp*$^{+/-}$ oocyte. Video 5 shows meiotic maturation in a *Hurp*$^{-/-}$ oocyte with polar body extrusion. Video 6 shows meiotic maturation in a *Hurp*$^{-/-}$ oocyte with prolonged metaphase I. Video 7 shows GFP-HURP overexpression. Video 8 shows mitosis in control U2OS cells overexpressing PLK4. Video 9 shows mitosis in HURP-depleted U2OS cells overexpressing PLK4. Online supplemental material is available at http://www.jcb.org/cgi/content/full/jcb.201005065/DC1.

We thank Hiro Ohkura, Julien Dumont, and Marie-Emilie Terret for critical reading of the manuscript. We are grateful to Anna Kouznetsova for help with chromosome spreads. We thank Erich Nigg for providing doxycycline-inducible PLK4-overexpressing U2OS cells.

M. Breuer is a recipient of a Ligue Nationale Contre le Cancer doctoral fellowship. M. Kwon is a recipient of a Special Fellow Award of the Leukemia and Lymphoma Society. S. Brunet is an Institut National de la Santé et de la Recherche Médicale fellow. This work was supported by grants from the Ligue Nationale Contre le Cancer (EL/2009/LNCC to M.-H. Verlhac), the Agence Nationale pour la Recherche (ANR08BLAN-0136-01 to M.-H. Verlhac), and the National Health Research Institutes (NHRI-EX99983 7NI to T.-F. Tsai).

Submitted: 14 May 2010
Accepted: 22 November 2010

References

Azoury, J., K.W. Lee, V. Georget, P. Rassinier, B. Leader, and M.-H. Verlhac. 2008. Spindle positioning in mouse oocytes relies on a dynamic meshwork of actin filaments. *Curr. Biol.* 18:1514–1519. doi:10.1016/j.cub.2008.08.044

Brunet, S., and B. Maro. 2007. Germinal vesicle position and meiotic maturation in mouse oocyte. *Reproduction.* 133:1069–1072. doi:10.1530/REP-07-0036

Brunet, S., A.S. Maria, P. Guillaud, D. Dujardin, J.Z. Kubiak, and B. Maro. 1999. Kinetochore fibers are not involved in the formation of the first meiotic spindle in mouse oocytes, but control the exit from the first meiotic M phase. *J. Cell Biol.* 146:1–12. doi:10.1083/jcb.146.1.1

Colombié, N., C.F. Cullen, A.L. Brittle, J.K. Jang, W.C. Earnshaw, M. Carmena, K. McKim, and H. Ohkura. 2008. Dual roles of Incenp crucial to the assembly of the acentrosomal metaphase spindle in female meiosis. *Development.* 135:3239–3246. doi:10.1242/dev.022624

Dumont, J., S. Petri, F. Pellegrin, M.-E. Terret, M.T. Bohnsack, P. Rassinier, V. Georget, P. Kalab, O.J. Gruss, and M.-H. Verlhac. 2007. A centriole- and RanGTP-independent spindle assembly pathway in meiosis I of vertebrate oocytes. *J. Cell Biol.* 176:295–305. doi:10.1083/jcb.200605199

Fitzharris, G. 2009. A shift from kinesin 5-dependent metaphase spindle function during preimplantation development in mouse. *Development.* 136:2111–2119. doi:10.1242/dev.035089

Godinho, S.A., M. Kwon, and D. Pellman. 2009. Centrosomes and cancer: how cancer cells divide with too many centrosomes. *Cancer Metastasis Rev.* 28:85–98. doi:10.1007/s10555-008-9163-6

Kleylein-Sohn, J., J. Westendorf, M. Le Clech, R. Habedanck, Y.D. Stierhof, and E.A. Nigg. 2007. Plk4-induced centriole biogenesis in human cells. *Dev. Cell.* 13:190–202. doi:10.1016/j.devcel.2007.07.002

Koffa, M.D., C.M. Casanova, R. Santarella, T. Köcher, M. Wilm, and I.W. Mattaj. 2006. HURP is part of a Ran-dependent complex involved in spindle formation. *Curr. Biol.* 16:743–754. doi:10.1016/j.cub.2006.03.056

Kubiak, J.Z., M. Weber, G. Géraud, and B. Maro. 1992. Cell cycle modification during the transitions between meiotic M-phases in mouse oocytes. *J. Cell Sci.* 102:457–467.

Kudo, N.R., K. Wassmann, M. Anger, M. Schuh, K.G. Wirth, H. Xu, W. Helmhart, H. Kudo, M. McKay, B. Maro, et al. 2006. Resolution of chiasmata in oocytes requires separase-mediated proteolysis. *Cell.* 126:135–146. doi:10.1016/j.cell.2006.05.033

Kwon, M., S.A. Godinho, N.S. Chandhok, N.J. Ganem, A. Azioune, M. Thery, and D. Pellman. 2008. Mechanisms to suppress multipolar divisions in cancer cells with extra centrosomes. *Genes Dev.* 22:2189–2203. doi:10.1101/gad.1700908

Liang, Z.Y., M.A. Hallen, and S.A. Endow. 2009. Mature *Drosophila* meiosis I spindles comprise microtubules of mixed polarity. *Curr. Biol.* 19:163–168. doi:10.1016/j.cub.2008.12.017

Mailhes, J.B., C. Mastromatteo, and J.W. Fuseler. 2004. Transient exposure to the Eg5 kinesin inhibitor monastrol leads to syntelic orientation of chromosomes and aneuploidy in mouse oocytes. *Mutat. Res.* 559:153–167.

Reis, A., H.Y. Chang, M. Levasseur, and K.T. Jones. 2006. APCcdh1 activity in mouse oocytes prevents entry into the first meiotic division. *Nat. Cell Biol.* 8:539–540. doi:10.1038/ncb1406

Sawin, K.E., K. LeGuellec, M. Philippe, and T.J. Mitchison. 1992. Mitotic spindle organization by a plus-end-directed microtubule motor. *Nature.* 359:540–543. doi:10.1038/359540a0

Schuh, M., and J. Ellenberg. 2007. Self-organization of MTOCs replaces centrosome function during acentrosomal spindle assembly in live mouse oocytes. *Cell.* 130:484–498. doi:10.1016/j.cell.2007.06.025

Schuh, M., and J. Ellenberg. 2008. A new model for asymmetric spindle positioning in mouse oocytes. *Curr. Biol.* 18:1986–1992. doi:10.1016/j.cub.2008.11.022

Silljé, H.H., S. Nagel, R. Körner, and E.A. Nigg. 2006. HURP is a Ran-importin beta-regulated protein that stabilizes kinetochore microtubules in the

vicinity of chromosomes. *Curr. Biol.* 16:731–742. doi:10.1016/j.cub.2006.02.070

Srayko, M., E.T. O'Toole, A.A. Hyman, and T. Müller-Reichert. 2006. Katanin disrupts the microtubule lattice and increases polymer number in *C. elegans* meiosis. *Curr. Biol.* 16:1944–1949. doi:10.1016/j.cub.2006.08.029

Terret, M.-E., C. Lefebvre, A. Djiane, P. Rassinier, J. Moreau, B. Maro, and M.-H. Verlhac. 2003a. DOC1R: a MAP kinase substrate that control microtubule organization of metaphase II mouse oocytes. *Development.* 130:5169–5177. doi:10.1242/dev.00731

Terret, M.-E., K. Wassmann, I. Waizenegger, B. Maro, J.-M. Peters, and M.-H. Verlhac. 2003b. The meiosis I-to-meiosis II transition in mouse oocytes requires separase activity. *Curr. Biol.* 13:1797–1802. doi:10.1016/j.cub.2003.09.032

Tsai, C.Y., C.K. Chou, C.W. Yang, Y.C. Lai, C.C. Liang, C.M. Chen, and T.F. Tsai. 2008. Hurp deficiency in mice leads to female infertility caused by an implantation defect. *J. Biol. Chem.* 283:26302–26306. doi:10.1074/jbc.C800117200

Tsou, A.P., C.W. Yang, C.Y. Huang, R.C. Yu, Y.C. Lee, C.W. Chang, B.R. Chen, Y.F. Chung, M.J. Fann, C.W. Chi, et al. 2003. Identification of a novel cell cycle regulated gene, HURP, overexpressed in human hepatocellular carcinoma. *Oncogene.* 22:298–307. doi:10.1038/sj.onc.1206129

Tsurumi, C., S. Hoffmann, S. Geley, R. Graeser, and Z. Polanski. 2004. The spindle assembly checkpoint is not essential for CSF arrest of mouse oocytes. *J. Cell Biol.* 167:1037–1050. doi:10.1083/jcb.200405165

Verlhac, M.-H., C. Lefebvre, P. Guillaud, P. Rassinier, and B. Maro. 2000. Asymmetric division in mouse oocytes: with or without Mos. *Curr. Biol.* 10:1303–1306. doi:10.1016/S0960-9822(00)00753-3

Walczak, C.E., I. Vernos, T.J. Mitchison, E. Karsenti, and R. Heald. 1998. A model for the proposed roles of different microtubule-based motor proteins in establishing spindle bipolarity. *Curr. Biol.* 8:903–913. doi:10.1016/S0960-9822(07)00370-3

Wignall, S.M., and A.M. Villeneuve. 2009. Lateral microtubule bundles promote chromosome alignment during acentrosomal oocyte meiosis. *Nat. Cell Biol.* 11:839–844. doi:10.1038/ncb1891

Wong, J., and G. Fang. 2006. HURP controls spindle dynamics to promote proper interkinetochore tension and efficient kinetochore capture. *J. Cell Biol.* 173:879–891. doi:10.1083/jcb.200511132

Yang, G., B.R. Houghtaling, J. Gaetz, J.Z. Liu, G. Danuser, and T.M. Kapoor. 2007. Architectural dynamics of the meiotic spindle revealed by single-fluorophore imaging. *Nat. Cell Biol.* 9:1233–1242. doi:10.1038/ncb1643

Yang, G., L.A. Cameron, P.S. Maddox, E.D. Salmon, and G. Danuser. 2008. Regional variation of microtubule flux reveals microtubule organization in the metaphase meiotic spindle. *J. Cell Biol.* 182:631–639. doi:10.1083/jcb.200801105

Yao, Z., and L. Mishra. 2009. Cancer stem cells and hepatocellular carcinoma. *Cancer Biol. Ther.* 8:1691–1698.